World Journal of Applied Chemistry
2017; 2(2): 34-47
http://www.sciencepublishinggroup.com/j/wjac
doi: 10.11648/j.wjac.20170202.11

On the Water Electrolysis with Photovoltaic Solar Energy for Hydrogen Production

A. Benghnia*, B. Nabil, R. Ben Slama, B. Chaouachi

Research Unit: Environment Catalyzes and Process Analysis, National School of Engineers of Gabes (ENIG), University of Gabes, Gabes, Tunisia

Email address:

afefbenghnia@hotmail.fr (B. Afef)

*Corresponding author

To cite this article:

A. Benghnia, B. Nabil, R. Ben Slama, B. Chaouachi. On the Water Electrolysis with Photovoltaic Solar Energy for Hydrogen Production. *World Journal of Applied Chemistry.* Vol. 2, No. 2, 2017, pp. 34-47. doi: 10.11648/j.wjac.20170202.11

Received: October 31, 2016; **Accepted**: December 29, 2016; **Published**: March 10, 2017

Abstract: In this paper we investigated the parameters determining the performance of hydrogen production by using the solar water electrolysis system (SWES), without the need of high additional electrical energy. The electrolyte after and before using in solar electrolysis was described to understand the mechanism responsible on the hydrogen production enhancement. Additionally, the employed electrolyte (deposit) was characterized by FT-IR, UV-visible and electrochemical impedance spectroscopy. As results the salt addition can obtained 40% more hydrogen efficiency. Also the pH values that varied between 3 to 6 and 8.5 to 12 could further improve hydrogen yield. The deposit provided a discriminate environment which is proposed to be responsible for the hydrogen production improvement. In addition, hydroxyl ions are mainly transported through the exchange anion, to maintain charge neutrality, and thus the anode and cathode electrode resulting in a low transport resistance. This can be assumed that the proton transport facilitated by water permeation can lower the transport resistance, and consequently increase hydrogen production.

Keywords: Solar Electrolysis, Hydrogen Production, Deposit, Electrochemical Impedance Spectroscopy

1. Introduction

These days, there is a great concern regarding the depletion of fossil oil reserves and the pollution caused by the growing demand for energy generation. In this way, a large-scale substitution of petroleum-based fuels as well as improved efficiency in energy conversion is required. In this context, fuel cells for mobile and stationary applications are highly valued due to their high theoretical efficiency and only steam as by product [1, 2].

Hydrogen is widely recognized as an alternative portable energy medium to fossil fuels. It can be utilized for road transport applications presenting high energy efficiencies in combination with a proton exchange membrane fuel cell with zero emissions at the point of use [3]. Despite the vast potential of the use of hydrogen as an energy vector in the so-called hydrogen economy, its widespread implementation is currently limited by the capacity limitations of current hydrogen storage technologies and by the safety issues associated with its storage and transportation [3, 4].

Although the water splitting process used to simultaneously generate hydrogen and oxygen has been demonstrated by the utilization, the technology is not mature enough to bring it to demonstration level. Much fundamental research remains to be done [5]. A long sought goal of energy research has been the search for a method to produce hydrogen fuel economically by splitting water using sunlight as the primary energy source. One of the main domains of solar energy research concerns the development of a process for the production of solar fuels. Among the solar fuel candidates, hydrogen holds a pre-eminent position because of its high energy content, environmental compatibility and ease of storage and distribution. The different approaches for splitting water have been summarized by Bockris as follows: electrolysis, plasmolysis, magnetolysis, thermal approach (direct, catalytic and cyclic decomposition of water, as well as magmalysis), use of light (photosensitized decomposition using dyes, plasmainduced photolysis, photoelectrolysis, photo-aided electrolysis, the indirect path towards hydrogen by photoelectrolysis: the photoelectrochemical reduction of CO_2 and photovoltaic electrolysis), biocatalytic

decomposition of water, radiolysis and other approaches [6].

Hydrogen is used as a fuel and in the future, the role of hydrogen may become more important, as some researchers suggest that the world's energy systems may undergo a transition to an era in which the main energy carriers are hydrogen and electricity [7, 8]. The production of hydrogen has been identified as in need of substantial research [9].

The status of research, development and demonstration of energetic solar hydrogen systems and their components were presented, including both scientific and technical aspects. Solar hydrogen is a clean energy carrier. Electrolytic hydrogen is made from water and becomes water again. Hydrogen obtained from solar energy (solar hydrogen) is ecologically responsible along its entire energy conversion chain. At only one link of the chain can a pollutant, nitrogen oxide, arise; and this occurs only if the hydrogen is not recombined with pure oxygen, but using air as an oxidant, such as in reciprocating piston engines or gas turbines on board automobiles or aircraft.

In this field, water electrolysis is one of the most important industrial processes for hydrogen production today, and is expected to become even more important in the future. As example, solar water electrolysis system (SWES) is an emerging "green" technology for hydrogen production from various types of waste materials, such as wastewater and other renewable resources. Electrons travel through external circuit to the cathode where H_2 is produced using protons in the solution. In order to produce hydrogen at the cathode from the combination of these protons and electrons, SWES require an externally supplied voltage under an assisted condition of pH, temperature, and pressure. However, SWES require relatively low energy input (1.23 e 1.8 V). Recently, a significant number of researchers have reported that the performance of water electrolysis is greatly influenced by several factors, such as initial pH, temperature [10, 11], electrolyte solution [12-15], substrates and anode surface area [16-18], electrode materials and electrode spacing [19, 20], cell internal and external resistance [21-24], and activated sludge concentration [25]. This is done by the input of a voltage via a solar power supply. It was then confirmed that the water permeation across the membrane induced by the osmotic pressure difference between the anode and cathode chambers, can expedite proton transport into the cathode chamber, thereby decreasing the pH imbalance.

On the other hand, the internal resistance, which consists of ohmic, charge transfer, and mass transfer resistances, increases the required voltage to be applied and inhibits performance in bioelectrochemical systems [26]. Because the internal resistance is an intrinsic property, it cannot be removed though it can be reduced depending on the membrane types [27]. Unfavorable ionic transport across the membrane can result in a high transport resistance, and ultimately decreasing the hydrogen production rate in [28]. Furthermore, [29] reported that hydrogen production can be enhanced by exchanging a cation exchange membrane for an anion exchange membrane due to the decrease in internal resistance [29]. Hydroxyl ions are mainly transported through the anion exchange membrane, to maintain charge neutrality, resulting in a low transport resistance [30, 31]. Indeed, it can be assumed that the proton transport facilitated by water permeation can lower the transport resistance, and consequently increase hydrogen production.

Of these factors, cathode material type with the high performance is the most important factor in the performance of water electrolysis where H_2 as well as other value-added chemical compounds are produced. According to a number of studies, noble metals such as platinum (Pt), copper (Cu), aluminum (Al) are typically used as cathode in water electrolysis studies.

The focus of this study was to quantify the characteristics of the photovoltaic panel (PV) and the electrolyzer in order to improve the hydrogen production. Different factors are affected, which are going to be discussed in the following sections of this paper. In addition, requirements for successful hydrogen production can therefore be summarized as follows; create the environmental conditions for the formation of produced hydrogen, discuss the change between pH after and before H_2 production and characterize the deposit electrolysis for the development of hydrogen producing organisms.

For this work, we used an integrated photovoltaic pane (PV) and electrolyzer design to emulate a solar water electrolysis system (SWES). Also, these integrated systems allow us to study the issues involving the effects of current density, solar intensity variability, and salt concentration on the overall efficiency for hydrogen production.

2. Methods and Materials

2.1. Electrolyzer Description and Operation

A large single-chamber (1000mL) was used to carry out the experiments. A copper fiber was used as anode ($4.8m^2$) and a cathode ($4.8m^2$) was made with aluminum. The electrode spacing was 30 mm between the anode/cathode electrodes, and a rubber gasket installed with the membrane to allow it to be tightened.

Both electrodes were arranged concentrically with the cathode in the outer perimeter, so that all ends of the anode were at the same distance from the cathode. The electrolyzer operated in batch mode, with constant agitation and an applied potential of 1.2 V between anode and cathode. The medium used (for different pH values and salt concentration) was operated with the addition of H_2SO_4, NaCl and NaOH (Sigma-Aldrich, USA). Afterwards, the electrolyte was placed on the electrolyzer to produce the gas like hydrogen.

The photovoltaic panel (PV) was the basic unit that converts light energy into electrical energy. The PV is formed by 36 polycrystalline silicon cells, supplying a current and voltage of 3.4 and L5V respectively. In order to improve the resources (adapting the desired voltage), the used PV was protected by regulators and converters Figure 1. Here, the aims of the regulators were to prevent the overload and the discharges of battery. Also, the regulators can protect the reversals polarity and solar polarity of battery.

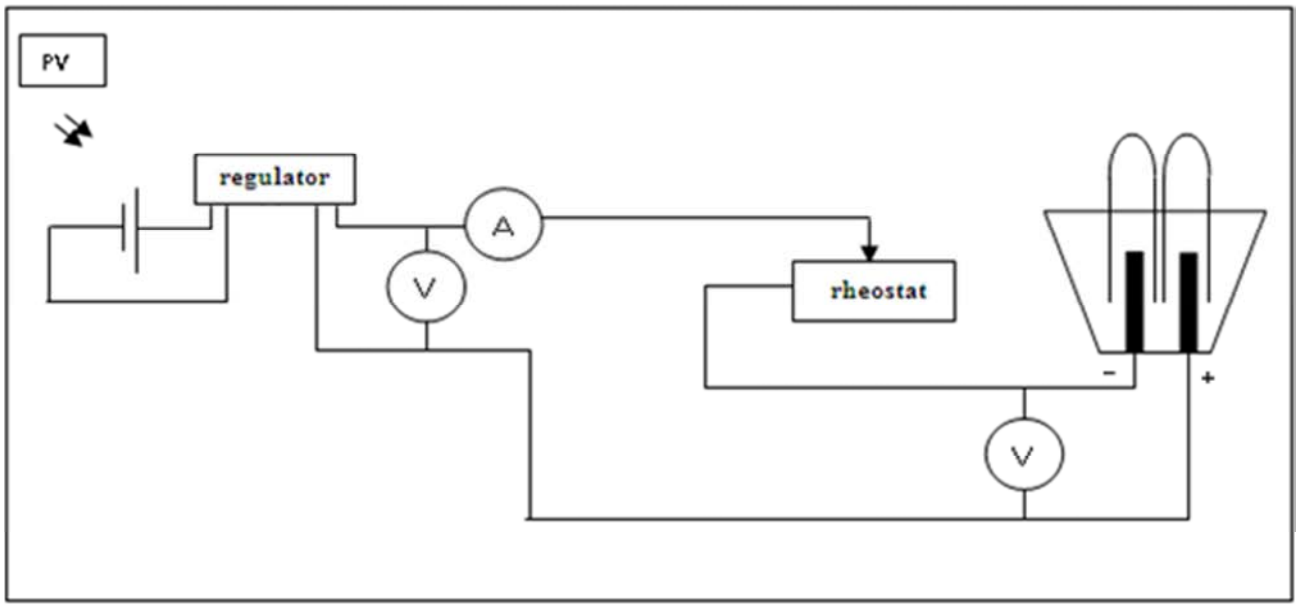

Figure 1. *Conception of the used solar water electrolysis system.*

2.2. Hydrogen Production

Solar water electrolysis tests were conducted using an electrolyzer connected to the generator with highest voltage U = 2 V and gradually decrease. The electrodes are separated by an ion-conducting electrolyte which allows ionic transfer between the electrodes. During this process, the electric energy supplied to the system is converted into chemical energy as hydrogen.

The water electrolysis tests were conducted at room temperature using an aqueous solution as electrolyte, which results in splitting water molecules into H_2 and oxygen (O_2). Hydrogen produced by electrolysis of water is of relatively high quality, as no carbon or nitrogenous compounds are generated in the process. The electrolyte for different pH values and salinity degrees were run for each of these solutions. Also, hydrogen productions were measured, depending on the case; the electrochemical half-reactions that occur at each electrode are different.

The hydrogen production tests are conducted to operate the hydrogen production efficiency, hydrogen production flow, absorbed power and the consumed electrical energy per volume unit Table A1.

2.3. Chemical Analysis

Deposit and powder of this deposit were analyzed by i; FT-IR spectroscopy using a KBr cell Fourier transformed IR equipment and infrared spectroscopy (NICOLET IR200), with wave ranged from 4000 to 400 cm^{-1}, ii; UV-VISIBLE spectrophotometer used to have more information on the different electrolytes (SHIMADZU, UV-1650PC) and iii; the pH of the electrolyte was checked at the start and end point of each step using a pH meter (Orion, USA) (Figure 2).

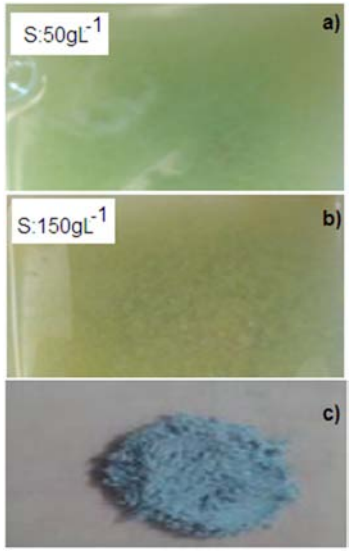

Figure 2. *Deposit image with different salinity values (a), (b) and deposit powder (c).*

2.4. Electrochemical Impedance Spectroscopy (EIS) Measurement

A potentiostat (PGSTAT302N, Autolab, Netherlands) was used to measure the impedance under open circuit voltage conditions of the electrolysis deposit. EIS was conducted over a frequency range of 10 mHz –1 kHz, stack potential (Ag/AgCl reference electrodes) and a sinusoidal amplitude of 10 mV measured using a frequency response analyser. Impedance analyses were performed under two electrode systems where the working electrode is connected to the cathode and reference electrodes is connected to the anode in which the cell voltage.

3. Results and Discussion

3.1. Characteristics of the Electrolyzer and Photovoltaic Panel

The characteristics curve of the electrolyzer is shown in Figure 3, allows us to determine the value of the open circuit voltage (V_{oc}) to start the electrolysis. This curve varies according to the electrolyzer, and its surface which can limit the progress of the hydrogen composition reaction recorded by [32]. Thus, the surveys tell us that the trigger voltage electrolysis was 18 V and 1.50 A as intensity. This reference determine for the modeling, the power required by the electrolyzer.

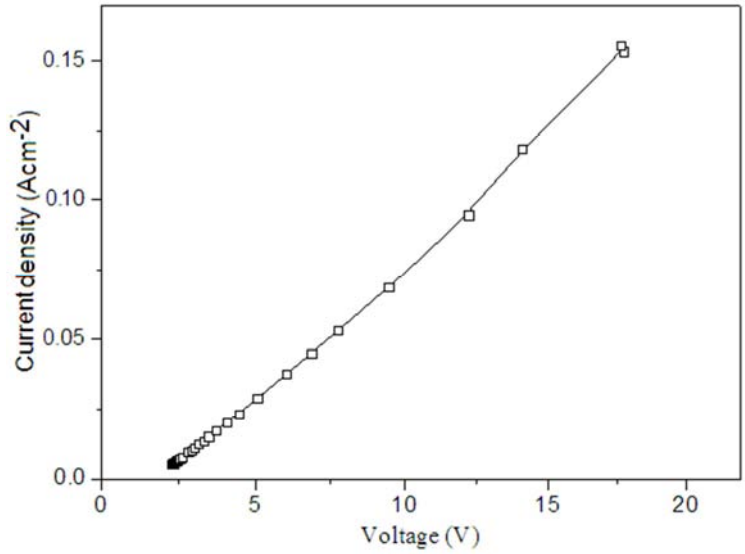

Figure 3. *Characteristic curve of the electrolyzer.*

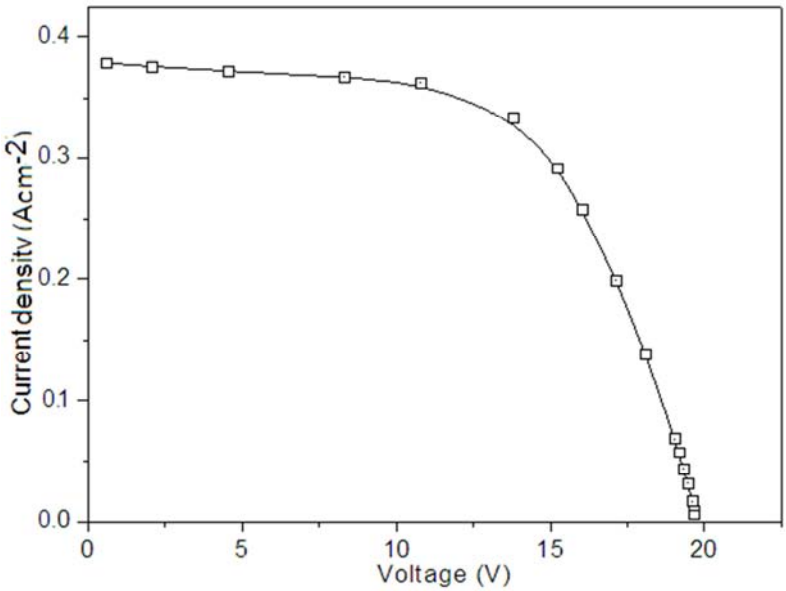

Figure 4. *Characteristic curve of the PV.*

On the other hand, the characteristic of the PV is shown in Figure 4, which reflects its energy behavior under the influence of incident radiation, temperature and load. The experiment is carried out under conditions known as 'natural' as follows: direct sunlight and not in halogen lamp with variable power. In fact, for the first steps, the module is fixed in a position and an orientation with an inclination of 35° to the horizontal. As result, choose among the measurements at a maximum variation of solar radiation, the V_{oc} varied between 18 and 20 V. Additionally, the short-circuiting varies according to sunlight. Indeed, the operating point is the intersection of the PV and electrolyzer curve [33]. Graphically discloses the operating point at the following coordinates (17.92 V; 1.50 A).

3.2. Electrolyzer Performance

Optimization of design parameters such as the height (h) between the electrode and the test tube were operated in terms of hydrogen yield in the electrolyzer at the applied voltages and current of 17 V and 1.5 A, respectively. The

height can enhance the performance of the hydrogen production and appeared as an important parameter to control the hydrogen production. Figure 5 reported the results of some tests at different heights. As seen the increases in the efficiency depended to the height and reaches a value of 3.5% when h = 3 cm and was proportional to the distance between the test tube and the electrode.

At 17 V, the current densities of the cathodes decreased slightly with the decrease of height getting larger (0.5 ± 0.05 A m^{-2} for h=3cm vs. 0.16 ± 0.05 A m^{-2} for h=1cm), which could result from the larger electrochemically area of electrolyzer.

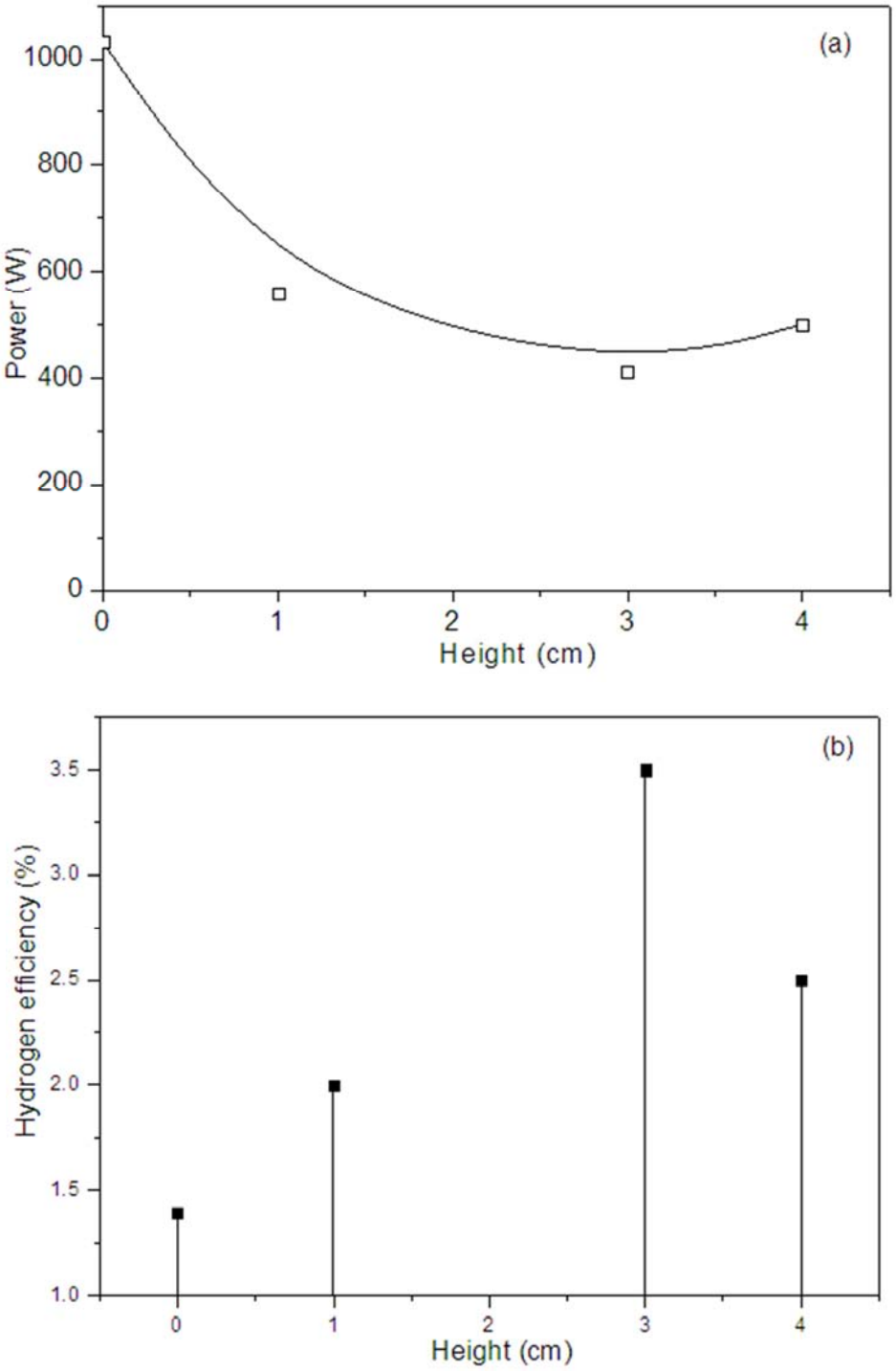

Figure 5. *Variation of the used power (a) and the hydrogen efficiency (b) at different height.*

Therefore, the measuring current has been increased by increasing h Figure 6 and above h=3cm current values decrease. This result is due to the low contact between both test tube and electrode, where the maximum charge in the electrolyte is developed, thus decreased to enter the test tube. Here these results can be explained by the role of the water quantity in contact with the electrode where is limited only inset the test tube and attributed by the charge number in water.

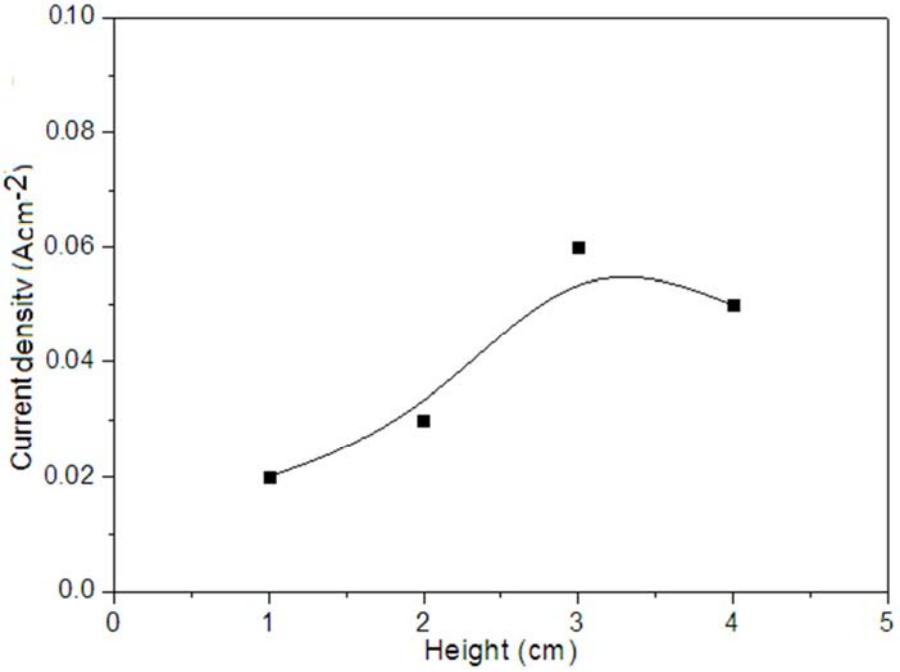

Figure 6. *Variation of the current as a function of the height.*

In this section, it is found out that the higher efficiency of water electrolysis arises in the smaller height between electrolyzer base and test tube, when current density is rather large. Summarizing these results, it can be explained by the hydrogen and oxygen bubbles densely pack at the upper part between electrolyzer base and test tube. It is also means the existence of optimum space depends on not only the current density but also the height of electrodes.

3.3. Hydrogen Production and Applied Energy

3.3.1. Hydrogen Gas Production

In order to quantify and improve the hydrogen efficiency from a direct conversion of PV/ electrolysis process. The solar cell must provide sufficient voltage to drive the water reactions, and also provide any additional voltage needed to overcome the overvoltage losses resulting from the hydrogen and oxygen evolution reactions.

The experiments, the area of the electrolyzer system and the PV is identical. These integrated systems allow us to study the issues involving the effects of current density, sunshine variability, salt concentration and pH value on the overall efficiency for hydrogen production.

Table 1 shows the hydrogen efficiency, and hydrogen flow at a fixed voltage input of 12 V and different salinity degrees. The hydrogen production efficiency was (25%) at 200gL^{-1} of NaCl and it was higher than some results presented in previous research.

Table 1. *Variation of hydrogen flow (Φ) and hydrogen efficiency (η) with different salinity values.*

Salinity (gL^{-1})	**5**	**50**	**70**	**90**	**110**	**130**	**150**	**170**	**190**	**210**
Φ (cm^3s^{-1})	0.10	0.45	0.20	0.15	0.11	0.09	0.19	0.30	0.39	0.4
η (%)	10	29	19	11	9	12	17	20	21	25

In this area, the salinity is strongly influenced the hydrogen production by solar water electrolysis. In fact, the current was increased with increases in salt concentration. It was shown in a previous study [34] that high salt concentration of input solution resulted in high conductivity of electrolyte. Herein, salinity was strongly correlated to the conductivity.

As a result, the addition of salt decreased the hydrogen production efficiency with increasing salinity of the medium. When the salinity increased the output increased, while the holding time decreases. This trend continues until a mass of salt is 50 g L^{-1}, around which the performance has a maximum value and where she uncrossed with the addition of NaCl. In addition, if we continue increased salinity, hydrogen efficiency and throughput decreases. From 130 g L^{-1}, both values began to grow with the addition of NaCl up to saturation of the electrolyte. This highlights the existence of changing the medium nature. Such pH difference was in accordance with the change of the current generations per tests in the electrolyzer. This change is resulted in more electrons reaching the cathode electrode and more hydroxide ion production due to oxygen reduction [35].

Figure A1 shown that electrolysis also decreased the pH value of electrolyte, thus this decrease was probably due to generations of chlorine gas, hypochlorous acid and hydrochloric acid. Total residual chlorine increased with increases of salt concentration and decreases of water flow. Increasing salt concentration increased chloride concentration of input water while decreasing flow rate increased residence time of the electrolyte in the electrolysis cells.

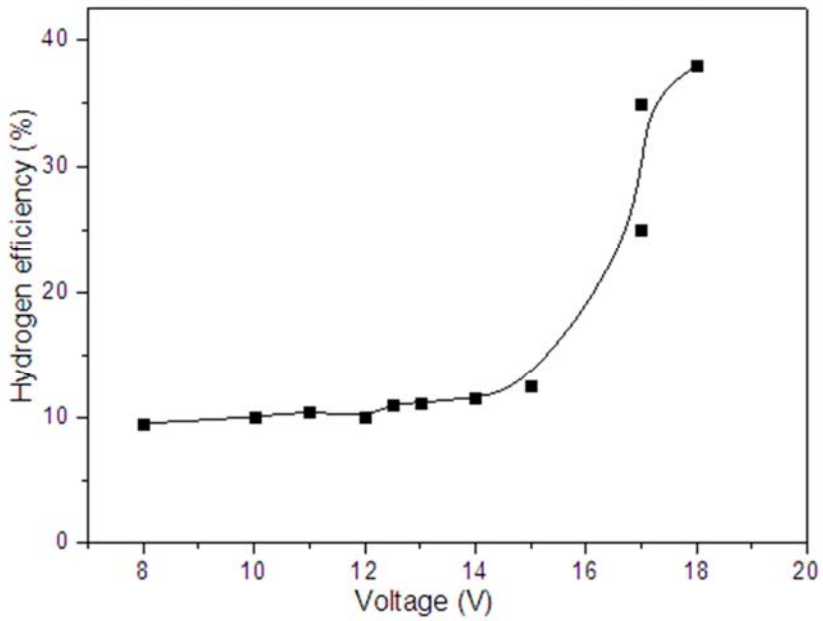

Figure 7. *Hydrogen efficiency at applied voltage.*

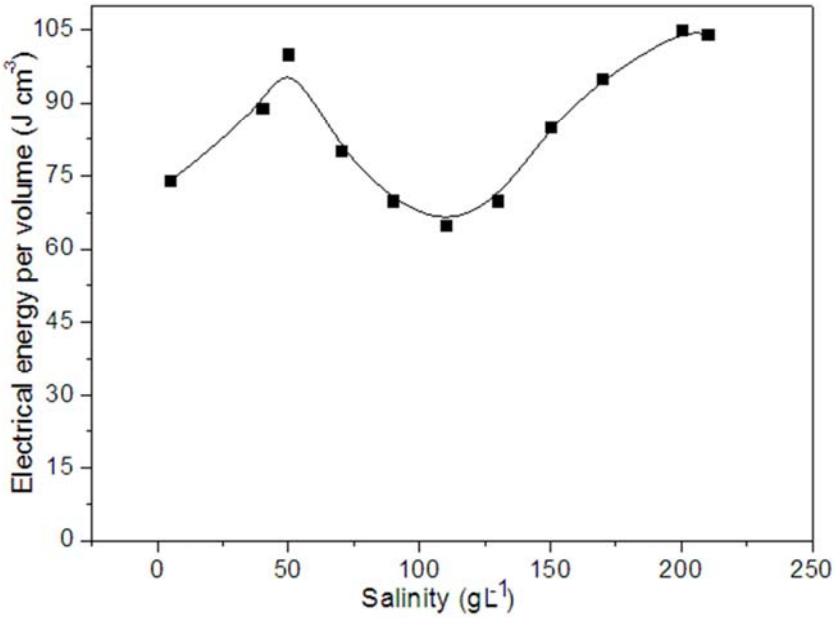

Figure 8. *Evolution of electrical energy as function of salinity.*

3.3.2. Energy Efficiency

Hydrogen production yield increased with the applied voltage of 10% at 8V to 40% at 18V (Figure 7). The production flow increased with the higher conductivity solution in part due to a decreased internal resistance. In contrast, results were reproducible when changing to any other applied potential for a voltage < 15 V.

The electrical energy efficiency for the conversion of water into hydrogen at different salinity degrees are shown in Figure 8. Under batch conditions, the overall energy decreased from 98 Jcm^{-3} at a 50gL^{-1} concentration of NaCl to 58 Jcm^{-3} at 70 gL^{-1}.

Using the results found this far in combination with literature values and we have assessed reasonable thickness between conductivity, pH values and degrees salinity values of the electrolyte to the improvement energy.

The variation of consumed energy per volume and the hydrogen flow with different pH values is reported in (Table A2). The salinity degrees and pH values variation offered the energy for the hydrogen production, while the input electricity provided the energy for the hydrogen production. The hydrogen production consumed 70 Jcm^{-3} in the salinity area around of 50 to 70 and 130 to 210gL^{-1}, which was much higher than that in the area of 50-130gL^{-1} (57 Jcm^{-3}. On the other term, the hydrogen production consumed more energy 118 Jcm^{-3}, 133 Jcm^{-3} for basic and acidic electrolyte

compared to the neutral medium 60.75 Jcm^{-3}, indicating that reaction mixture played an important role in boosting the performance of hydrogen production.

3.4. Deposit Characterization

3.4.1. FT-IR Analysis

Figure A2 shown the infrared spectra of the used electrolyte after and before hydrogen production. The band centered at about 3298 cm^{-1} and 1641 cm^{-1} associated to the stretching vibrations υOH, and the deformation vibration δOH, respectively. After hydrogen production the spectra shows a slight shift towards the low wavenumber with compared relative before production. Here, this result can be explained by the existing of interaction between chemical species and OH groups in electrolyte. Therefore, this difference indicate the metallic particles dispersion on electrolyte, which provides further evidence providing insights into strong interactions between hydrogen and oxygen [36].

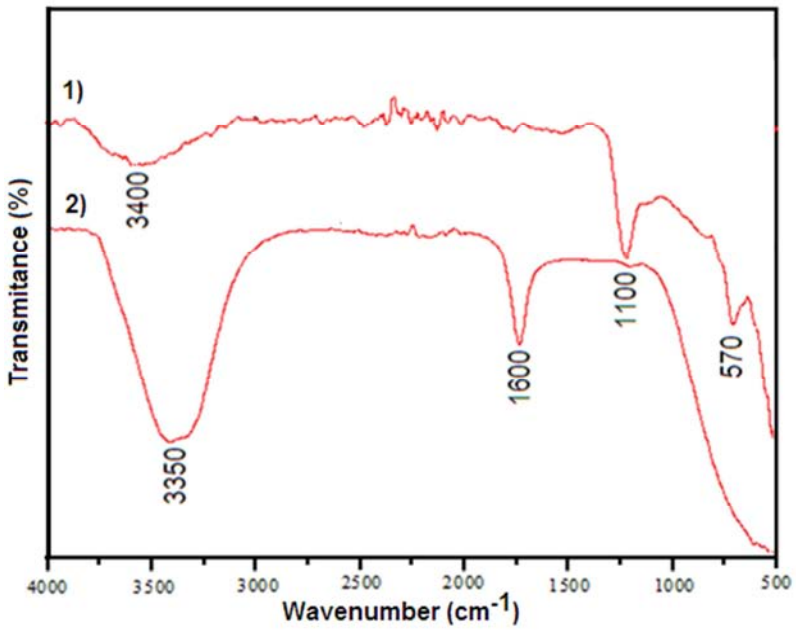

Figure 9. *Comparative FT-IR spectra of deposit powder (1) and electrolyte before solar electrolysis*

On the other hand, the infrared spectra recorded to the powder deposit samples and electrolyte after use (filing) are shown in Figure 9, reveals the presence of a band at 1600 cm^{-1} attributed to the deformation vibrations δOH for powder of deposit, while this band is largely shifted to lower wavelengths. Also, a broad absorption band around 3350 cm^{-1} associated to the stretching vibration υOH. A reduction of this band was signaled of the powder deposit that explained by drying the films in the open area. These results were confirmed the presence of free absorption band of OH groups at 3667 cm^{-1} [37, 38]. Thus the study by infrared spectroscopy confirms the presence of hydroxyl species in the film [39-41]. The lowest intensity as 600 and 445 cm^{-1} is attributed to stretching vibration of υCu-O is persisted for the powder which is not the case for the deposit before filtration

3.4.2. UV-visible Analysis

Figure 10 shows the UV spectrum of the electrolyte before and after hydrogen production, the only identifiable complex by UV-visible is $AlOH_3$ complex, which has an absorption band at 290 nm attributed to transitions load, and which caused the transfer of electrons promotes with a length difference of Al-OH bond. Among other things, this band is assigned to the electronic transition of the strong conjugation resulting hydroxyl group between electrolyte and electrodes.

The effect of the pH value was shown in Figure A3, which provides comparative studies of the UV-visible spectra of electrolyte for different pH values. The absorbance of all the samples having absorption bands around 220 nm, which is more intense to pH = 3, and which moves towards higher energy while increasing the pH value. This decrease can be explained by the exchange rate of existing charges in the electrolyte intensity of the transition which is significantly reduced. Contrary, for pH = 8, two bands are loaded at 320 and 360 nm due to the detected hydroxyl-compounds.

The effect of the salinity degrees value was shown in Figure A4, which prove the intensity variation of detected bands at 220 nm is higher for the masses of NaCl: 6 and 210 gL^{-1}, that explained by the development of acid-base game, while recording the band at 290 nm. However it is gone for other mass concentrations following dependence of the species disappearance.

3.4.3. Electrochemical Impedance Spectroscopy Measurement (EIS)

To insight into the influence of pH value on the electronic property of the deposit film, Figure 11 displays the Nyquist plots and the corresponded Bode diagrams of deposit. It can be seen that the Nyquist plots show a depressed semicircle, and the presence of the depressed semicircles is often referred to as frequency dispersion, which has been attributed to high roughness of the deposit surface [42, 43].

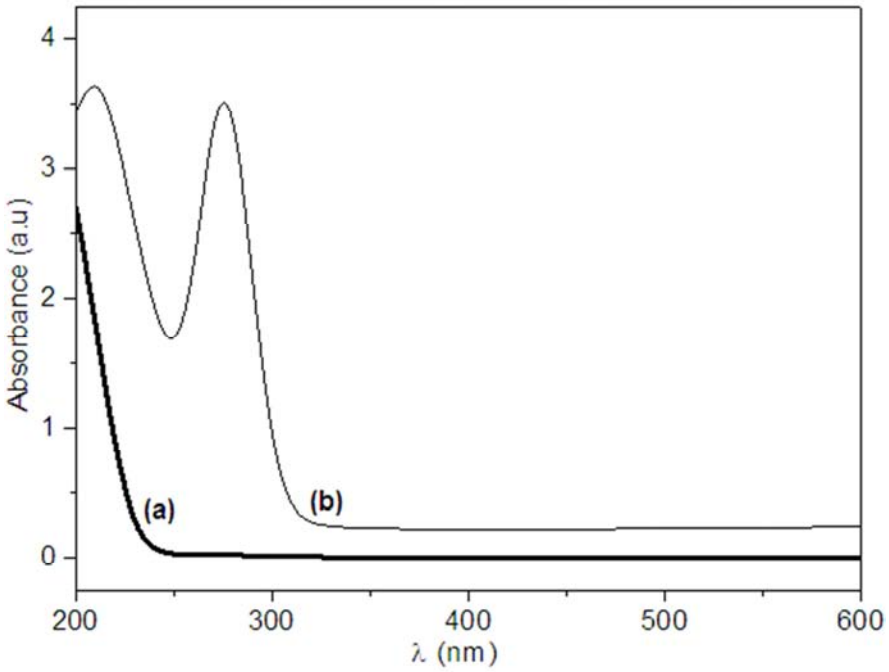

Figure 10. *UV–VIS spectra of the evolution of the absorption band for used electrolyte after and before solar electrolysis.*

In order to gain the quantitative explain of pH value on the electronic property of the deposit, the measured EIS are fitted by appropriate equivalent electron circuit.

Using the circuit the impedance spectrum is expected to comprise three hierarchically distributed time constants provided by Macdonald [44] (Figure A5) is used to fit the impedance, in which C represent the capacitive of the metallic electrode and deposit interface, CPE (constant phase element) represent the solution/ barrier interface and Rs is the deposit fime resistance.

A high resistance should result in high energy loss [45]. The resistance significantly increases with the increase in pH value. Therefore, the ohmic resistance played an important role in the performance of electrolyzer. It should be essential to effectively decrease the ohmic resistance for improving the current density, which needs further study. Here, this result can be contributed to resistive changing occurring at the metallic electrode and deposit interfaces. It can be seen from Figure 11 that the value of the resistance pH 10 is much higher than that of pH 3, it can be concluded that the increment of pH value can increase the resistance of the deposit and metallic electrode interface.

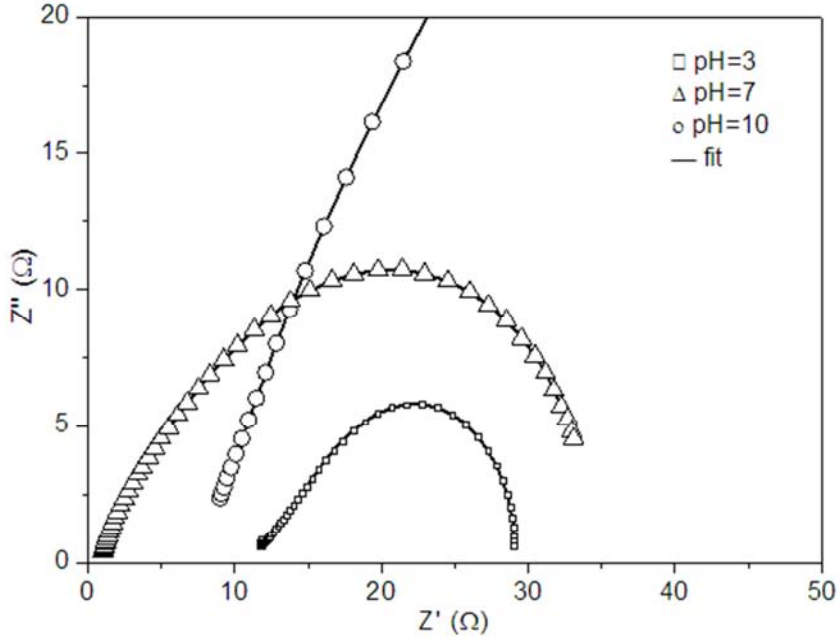

Figure 11. *Nyquist plot and their fitted data with different pH values.*

Figure 12 (a-b) show respectively, the variations of Z' and Z'' as a frequency function for different pH values. In fact, Z' values is quite high in the low frequency region, which is due to the free charges accumulation at the electrode-electrolyte interface. While for high frequencies, Z' tends towards values close to zero, which indicates the decrease in the material dielectric constant. Furthermore, Z'' factor has significant values at low frequencies and increases to another pH, but high frequency curves Z'' show similar behavior at different pH approaching zero.

4. Conclusions

This study intensively investigated the hydrogen production by solar water electrolysis system (SWES). The primary goal was to demonstrate the capability of SWES to produce hydrogen. When the applied voltage was 17 V, the electrolyzer can accomplished a hydrogen production efficiency of 40% at volumetric current density of 0.3 A m^{-2}.

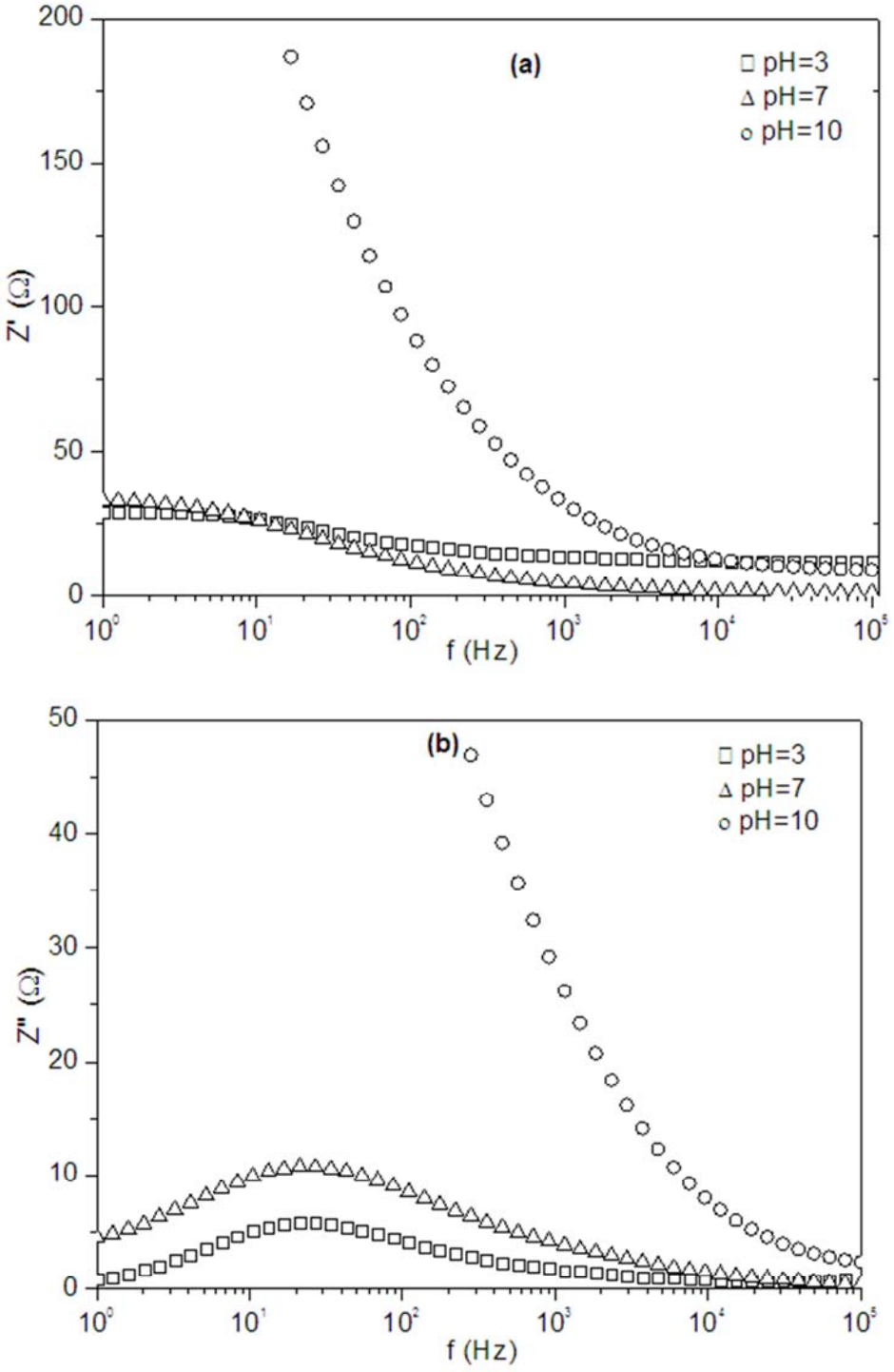

Figure 12. *Variation of the real (a) and imaginary (b) part of impedance as function of frequency with different pH values.*

These results demonstrate that H_2 production in the electrolyzer is seriously affected by the salinity degrees and pH values. Moreover, at higher and low concentration of NaCl, the hydrogen flow is improved and the activity decreased. Also the salinity has a strong effect in reducing the activation energy of the reaction such us for the salinity degrees around 70 to 130gL^{-1}. These results are accompanied by the presence of a deposit film. A combination of characterization methods to the deposit show that UV-visible spectra of the solution before and after the hydrogen production presents an absorption band at 290 nm assigned to transitions load, causing promoted electrons transfer. Infrared spectroscopy shows a shift in the OH absorption band which was a positive indicator of the metal particles interaction dispersed on the electrolyte. In the other hand, the study by complex impedance spectroscopy displayed that Nyquist diagrams saved a capacitive impedance loop and at high frequency domain followed by an inductive loop to the field of low frequencies and a capacitive behavior show the interface in the examined frequency range.

5. Supporting Information

5.1. Calculations

Table A1. *Parameters used in this study.*

Calculated parameters	Symbol	Formula
Hydrogen flow	Q	V/t (m^3s^{-1})
Absorptive power by the electrolyzer	Pa	U*I (w)
Consumed electric Energy	W	Pa*t in (J)
Hydrogen efficiency	η	PCI (Jkg^{-1})
Consumed Energy per volume	W/v	Pa*t/V = Pab/Q (Jcm^{-3}) Pa*t*22.4/V = ($KJmol^{-1}$)

Where; V is the volume of the test tube (m^3); t is the filling time of the tube (s); PCI is the lower calorific value of hydrogen = (119.9 10 6 JKg^{-1}); ρ is the density of hydrogen (0.09 Kgm^{-3}); I is the electrical current (A) and U is the tension (V).

5.2. Hydrogen Production

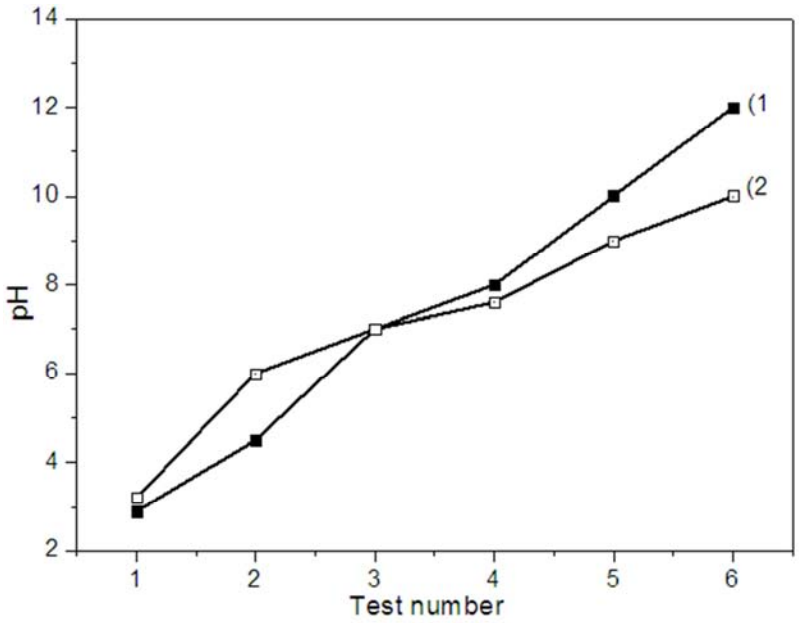

Figure A1. *Dependences of pH values before (1) and after (2) electrolysis.*

5.3. Consumed Energy

Table A2. *Hydrogen flow and consumed energy per volume with different pH values.*

pH	t (min)	I (A)	Φ (cm^3min^{-1})	W/V (Jcm^{-1})
2	18	0.66	4.44	133.65
3	33	0.25	2.42	92.81
6	45	0.12	1.77	60.75
10	30	0.30	2.66	101.25
12	15	0.70	5.33	118.12

5.4. Deposit Characterization

5.4.1. FT-IR Analysis

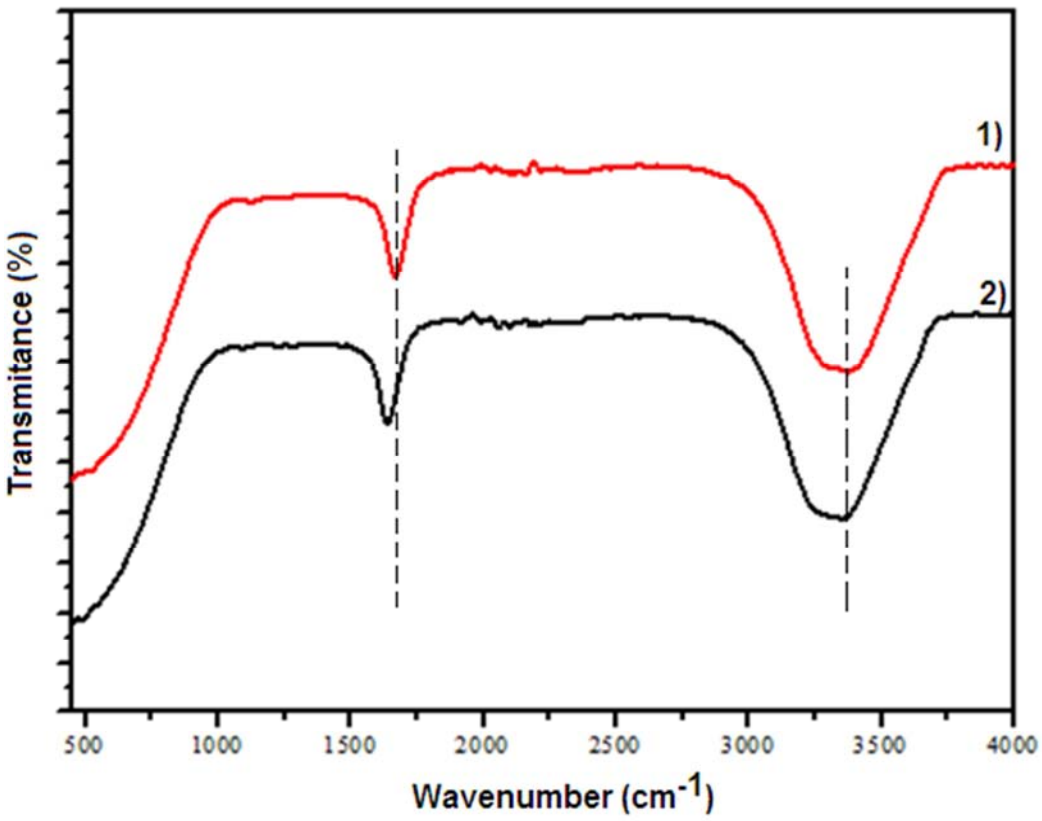

Figure A2. *FT-IR spectra of used electrolyte after (1) and before (2) solar electrolysis.*

5.4.2. UV-visible Analysis

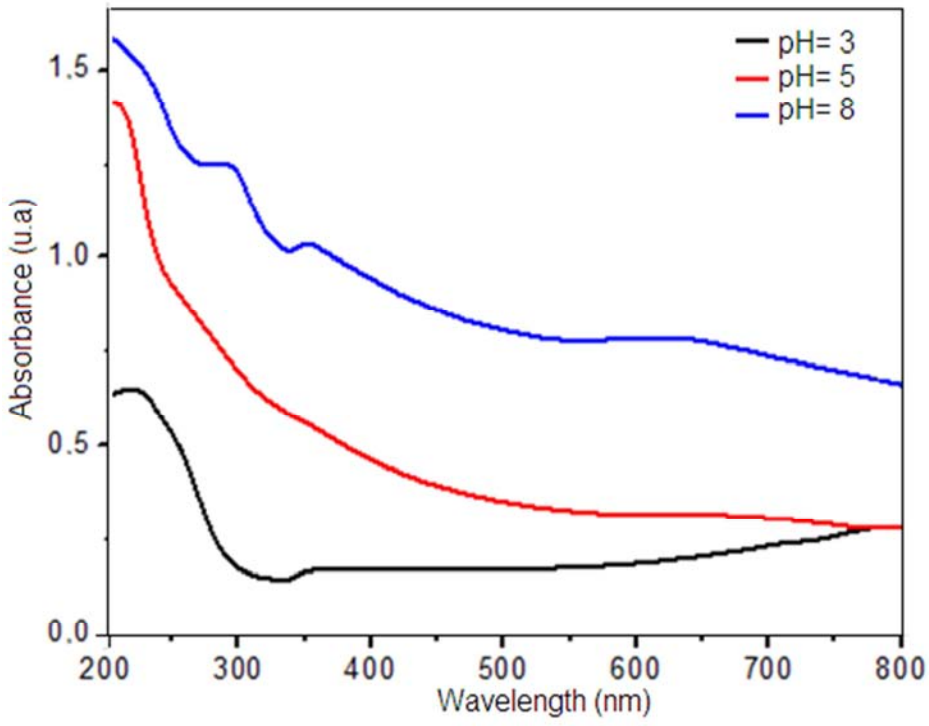

Figure A3. *Evolution of the absorption band for used electrolyte with different pH values.*

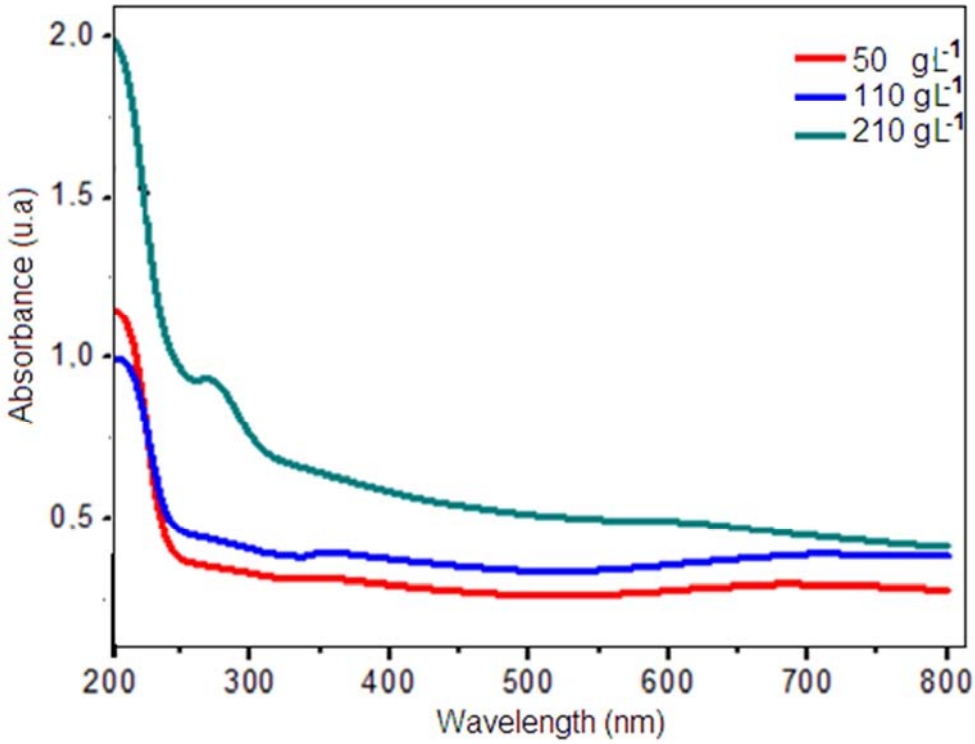

Figure A4. *Evolution of the absorption band for used electrolyte with different salinity values.*

5.4.3. Electrochemical Impedance Spectroscopy (EIS) Measurement

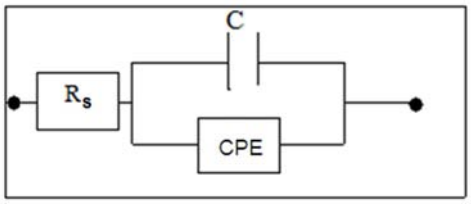

Figure A5. *Equivalent circuit model of the deposit compound.*

References

[1] Larminie J, Dicks A. Fuel cell systems explained. New York: Wiley, (2000).

[2] Dunn S. Int J Hydrogen Energy, 27 (2002) 235-64.

[3] Schlapbach L, Zuttel A. Nature, 414 (2001) 353-8.

[4] Suh MP, Park HJ, Prasad TK, Lim DW. Chem Rev, 112 (2012) 782-835.

[5] Serpone N, Lawless D, Terzian R. Solar Energy, 49 (1992) 221.

[6] Bockris JOM, Dandapani B, Cocke D, Ghoroghchian J. Int J Hydrogen Energy, 10 (1985) 79.

[7] Barbir, F., Plass, H. J. Jr. and Veziroglu, T. N., Int J Hydrogen Energy, 18 (1993) 87-195.

[8] Scott, D. S., Int J Hydrogen Energy, 18 (1993) 191-204.

[9] Hassmann, K. and Kuhne, H.-M., Primary energy sources for hydrogen production, Int J Hydrogen Energy, 18 (1993) 635-640.

[10] Kyazze G, Popov A, Dinsdale R, Esteves S, Hawkes F, Premier G, et al. Int J Hydrogen Energy, 35 (2010) 7716-22.

[11] Ribot-Llobet E, Nam J-Y, Tokash JC, Guisasola A, Logan BE. Int J Hydrogen Energy, 38 (2013) 2951-6.

[12] Merrill MD, Logan BE. J Power Sources, 191 (2009) 203-8.

[13] Nam J-Y, Logan BE. Int J Hydrogen Energy, 36 (2011) 15105-10.

[14] Nam J-Y, Logan BE. Int J Hydrogen Energy, 37 (2012) 18622-8.

[15] Yossan S, Xiao L, Prasertsan P, He Z. Int J Hydrogen Energy, 38 (2013) 9619-24.

[16] Cheng S, Logan BE. Proc Natl Acad Sci, 104 (2007) 18871-3.

[17] Darus L. Indo J Biotech, 16 (2011) 53-9.

[18] Croese E, Jeremiasse AW, Marshall IP, Spormann AM, Euverink GJ, Geelhoed JS,. Enzyme Microb Technol, 62 (2014) 67-75.

[19] Wang A, Liu W, Ren N, Zhou J, Cheng S. Int J Hydrogen Energy, 35 (2010) 13481-7.

[20] Selembo PA, Merrill MD, Logan BE. J Power Sources, 190 (2009) 271-8.

[21] Cheng S, Logan BE. Bioresour Technol, 102 (2011) 3571-4.

[22] Wang A, Liu W, Ren N, Cheng H, Lee D-J. Int J Hydrogen Energy, 35 (2010) 13488-92.

[23] Jung S, Regan JM. Appl Environ Microbiol, 77 (2011) 564-71.

[24] Lee MY, Kim KY, Yang E, Kim IS. Bioresour Technol, 187 (2015) 106-12.

[25] Chae KJ, Choi MJ, Kim KY, Ajayi FF, Chang IS, Kim IS. Environ Sci Technol, 43 (2009) 9525-30.

[26] ElMekawy, A., Hegab, H. M., Dominguez-Benetton, X., Pant, D., Bioresour. Technol. 142 (2013) 672–682.

[27] Kim, K.-Y., Chae, K.-J., Choi, M.-J., Yang, E.-T., Hwang, M. H., Kim, I. S., Chem. Eng. J. 218 (2013) 19–23.

[28] Liu, H., Logan, B. E.,. Environ. Sci. Technol. 38 (2004) 4040–4046.

[29] Sleutels, T. H. J. A., Hamelers, H. V. M., Rozendal, R. A., Buisman, C. J. N., Int. J. Hydrogen Energy 34 (2009) 3612–3620

[30] Werner, C. M., Logan, B. E., Saikaly, P. E., Amy, G. L., J. Membr. Sci. 428 (2013) 116–122.

[31] Zhang, F., Brastad, K. S., He, Z., Environ. Sci. Technol. 45 (2011) 6690–6696.

[32] R. Rozendal, H. Hamelers, G. Euverink, S. Metz, and C. Buisman, Int J Hydrogen Energy, vol. 31 (2006) 1632-40.

[33] P. Millet, F. Andolfatto and R. Durand, Int J Hydrogen Energy, 21 (1996) 87.

[34] S. Y. Hsu, Journal of Food Engineering, 60 (2003) 469–473.

[35] Min Su, Liling Wei, Zhaozheng Qiu, Gang Wang, Jianquan Shen, Journal of Power Sources 301 (2016) 29–34.

[36] Adrian. S, Claion. R, Spectro-chemical analysis, 18 (2013) 114 – 126.

[37] Rand. D, Dell. R, Hydrogen, RSC publishing (2008).

[38] Aníbal. M, Slavutsky. M, Bertuzzi. A, Margarita. A, María. G, García. N, A. Ochoa, 35 (2013) 270-278.

[39] del Arco. M, Trujillano. R, Rives. V, J, Chem, 8 (1998) 761.

[40] Uzunova. E, Klissurski. D, Mitov. I, Stefanov. P, J, Chem. Mater, 5 (1993) 576.

[41] Hansen. H. C. B, Koch. C. B, Taylor. R. M, J. Solid State Chem, 113 (1994) 46.

[42] Ju¨ ttner K. Electrochim Acta. 35 (1990) 1501.

[43] Ameer MA, Fekry AM, Taib Heakal FEI. Electrochim Acta (2004) 50: 43.

[44] Priyantha N, Jayaweera P, Macdonald DD, Sun A. J Electroanal Chem (2004) 572: 409.

[45] Sharma, M., Bajracharya, S., Gildemyn, S., Patil, S. A., Alvarez-Gallego, Y., Pant, D., Rabaey, K., Dominguez-Benetton, X., Electrochim. Acta 140 (2014) 191–208.